Transfer-matrix method for the complex band structure of superlattices

E. Ghahramani and J. E. Sipe
Department of Physics and Ontario Laser and Lightwave Research Centre, University of Toronto, Toronto, Ontario, Canada M5S 1A7
(Received 15 February 1989)

We demonstrate that a real-space transfer-matrix method can be used to directly evaluate the complex and real band structures of superlattices. The transfer-matrix method avoids the introduction of a supercell in the band-structure calculations. As a prototype we have used the direct space, minimal-basis linear combination of Gaussian orbitals method to evaluate the Hamiltonian and overlap-matrix elements. Our results for strained $(Si)_n/(Ge)_n$ (001) superlattices ($n=2-5$) are presented. We find all the above superlattices to have indirect band gaps. In particular, for $(Si)_4/(Ge)_4$ the lowest direct transition is at 1.38 eV. The results are in good agreement with recent experimental measurements.

I. INTRODUCTION

In recent years there has been much interest in calculating the band structure of superlattices, and not a little controversy over some of the results. The interest stems both from a fundamental concern with electronic structure of these novel materials and from a practical concern with the possibility of designing structures that exhibit desired optical or electronic properties. The controversy stems both from the difficulty in calculating the electronic properties of these complex structures and from the problems in growing these materials with sufficient ease so that a host of experiments on many well-characterized samples can be performed. A case in point is the strained $(Si)_n/(Ge)_n$ (001) superlattices ($n=2-6$) that have recently been studied.[1-8] For $n=4$, the majority view[1-5] is that the transition observed at 0.76 eV is indirect, but some researchers find it to be direct.[7,8]

In this paper we present a transfer-matrix method for calculating the complex band structure of superlattices. The method can be implemented within any approach based on a tight-binding description of the electronic states, ranging from empirical to *ab initio* self-consistent density-functional models. The difficulties associated with a "supercell" basis, which become particularly onerous as the size of the superlattice unit cell increases, are avoided: The size of the matrices which must be diagonalized in our approach is independent of the size of the unit cell of the superlattice. Further, the part of the complex band structure of the superlattice that would be useful in investigating, e.g., surface states localized at the interface between the superlattice and its substrate are found at the same time as the propagating electronic states are calculated.

In the transfer-matrix method we seek superlattice wave functions as linear combinations of two-dimensional Bloch states constructed from atomic orbitals on each atomic plane perpendicular to the superlattice axis **z**. We henceforth refer to these planes as "superlattice planes." Whereas usual band-structure calculations proceed by specifying the crystal momentum $\mathbf{k}=(k_x,k_y,k_z)$ and finding the wave-function energies E, we proceed by specifying the transverse wave vector $\mathbf{k}_t=(k_x,k_y)$ and the energy E, and determine k_z: For a fixed $\mathbf{k}_t$ and E, transfer matrices are constructed which relate the expansion coefficients of two-dimensional Bloch states on a given superlattice plane to those on previous planes. By multiplying an appropriate number of these matrices and using Bloch's theorem, an eigenvector equation is set up. The eigenvalues yield longitudinal wave-vector components k_z, real k_z specifying propagating states and complex k_z specifying complex bands with real wave-vector components (k_x,k_y) perpendicular to the superlattice axis; the eigenvectors give the expansion coefficients of the superlattice wave function. It is because the transfer matrices depend only on the range of interaction between orbitals on different planes, and on the number of orbitals used in the expansion, that the calculation is essentially independent of the size of the superlattice unit-cell size.

We note that Schülman *et al.*[9] have used a transfer-matrix method to evaluate the complex band structure of *bulk materials* within the framework of an empirical tight-binding model. They then use the complex state of bulk materials to obtain a real band structure for a superlattice made up of these materials. But their approach is quite different from ours. They make an initial guess at the energy of one of the superlattice states, and for this energy and for a fixed $\mathbf{k}_t$ transfer, matrices are constructed for each constituent bulk material using the bulk empirical matrix elements. The appropriate products of transfer matrices for each bulk material are diagonalized to obtain their complex band structures. The complex bulk states so obtained are used to construct a "*reduced Hamiltonian*" matrix for the superlattice, and the superlattice band structure is then obtained by diagonalizing this matrix. Since the energy is assumed in calculating the bulk complex states at the beginning, the procedure must be iterated until the assumed energy and the obtained energy are reasonably close. Brey *et al.*[10] have

pointed out that this method requires very lengthy calculations.

In our method we construct one set of transfer matrices directly for the superlattice, and obtain the complex band structure of the superlattice for a fixed $\mathbf{k}_t$ and any desired energy. Only one diagonalization is needed, namely that of the product transfer matrix. More importantly, we do not make a guess at the superlattice energy and, therefore, there is no iteration of energy. Further, the "*reduced Hamiltonian*" method produces only real bands, while we obtain complex bands of the superlattice itself.

The paper is organized as follows: In Sec. II we give a description of the transfer-matrix method for superlattices. To implement it requires an evaluation of Hamiltonian and overlap matrix elements. With an eye towards self-consistent calculations, we detail this evaluation in Sec. III for a linear combination of Gaussian orbitals (LCGO) expansion of both the atomic orbitals and the effective single-particle potential. This expansion allows for the analytic evaluation of matrix elements; in an *a priori* calculation the expansion coefficients would be modified after each calculation until self-consistency was achieved. In Sec. IV we present a sample calculation applying our method to the strained $(\mathrm{Si})_n/(\mathrm{Ge})_n$ series of superlattices. Since our main goal in this paper is to demonstrate the transfer-matrix method, we do not perform a self-consistent calculation. Instead, we simply use the semi-*ab initio* orbitals and effective potentials of bulk semiconductors to construct the superlattice orbitals and effective potentials. In this manner we do not do any fitting to the superlattice properties. The band gaps that result from the calculation should thus be identified with the observed transitions, as opposed to density functional calculations where the "band gaps" must be adjusted with quasiparticle corrections,[2,11] or more approximately by an upward shift in the conduction bands.[4,6,8] Despite the simple model used for calculating the matrix elements, it is gratifying to see how well our results agree with experimental results.[3,5] Our results and conclusions are given in Sec. V. For simplicity we only present the real bands found from our calculation. We plan to turn to applications involving the complex bands, as well as self-consistent calculation and the calculation of optical properties using this approach, in future publications.

II. TRANSFER-MATRIX FORMALISM FOR SUPERLATTICES

The transfer-matrix formalism for superlattices is similar to the formalism of Schülman *et al.*[9] for bulk materials. However, some of the details are different and, more importantly, the wave functions and Hamiltonian matrix elements in our approach refer to the superlattice. We outline the formalism below, relegating some of the algebraic details to the Appendix.

Let Λ index the atomic planes perpendicular to the superlattice axis direction ($\hat{\mathbf{z}}$), such that $\Lambda=0$ refers to the plane at the origin. We denote the ith orbital of an atom located in the Λth plane by $\Phi_{i\Lambda}(\mathbf{r}-d_\Lambda\hat{\mathbf{z}})$, where d_Λ is the distance between the Λth plane and the origin along $\hat{\mathbf{z}}$. A two-dimensional Bloch state for this orbital is constructed as follows:

$$\zeta_{i\Lambda}(\mathbf{r}-d_\Lambda\hat{\mathbf{z}})=\sum_{\mathbf{R}(\Lambda)} e^{i\mathbf{k}_t\cdot\mathbf{R}(\Lambda)}\Phi_{i\Lambda}(\mathbf{r}-\mathbf{R}(\Lambda)-d_\Lambda\hat{\mathbf{z}}) , \quad (2.1)$$

where the summation is over all the two-dimensional vectors $\mathbf{R}(\Lambda)$ pointing to the lattice sites in the Λth plane. The full two-dimensional Bloch state in the Λth plane, ψ_Λ, is given by

$$\psi_\Lambda(\mathbf{r}-d_\Lambda\hat{\mathbf{z}})=\sum_i C_i(\Lambda)\zeta_{i\Lambda}(\mathbf{r}-d_\Lambda\hat{\mathbf{z}}) , \quad (2.2)$$

where $C_i(\Lambda)$ are the expansion coefficients for the different orbital Bloch functions. Finally, the superlattice wave function is written in terms of these Bloch states as

$$\Psi(\mathbf{r})=\sum_\Lambda \psi_\Lambda(\mathbf{r}-d_\Lambda\hat{\mathbf{z}})=\sum_\Lambda\sum_i C_i(\Lambda)\zeta_{i\Lambda}(\mathbf{r}-d_\Lambda\hat{\mathbf{z}}) . \quad (2.3)$$

In order to find the $C_i(\Lambda)$ we require the wave function $\Psi(\mathbf{r})$ to satisfy the Schrödinger equation $\hat{H}\Psi(\mathbf{r})=E\Psi(\mathbf{r})$ which, in the nonorthonormal $\zeta_{i\Lambda}$ basis yields

$$\sum_\Delta\sum_j \int d\mathbf{r}[\zeta^*_{i\Lambda}(\mathbf{r})(\hat{H}-E)\zeta_{j\Lambda+\Delta}(\mathbf{r}-d_{\Lambda+\Delta}\hat{\mathbf{z}})]C_j(\Lambda+\Delta) =0 . \quad (2.4)$$

Defining the quantity in the square brackets to be $(H_{\Lambda,\Lambda+\Delta})_{ij}$, Eq. (2.4) can be rewritten as

$$\sum_\Delta\sum_j (H_{\Lambda,\Lambda+\Delta})_{ij}C_j(\Lambda+\Delta)=0 . \quad (2.5)$$

In principle, the outer sum runs over all the planes in the superlattice. However, at some point the contributions of the far planes become negligible and one can truncate the sum. Let us restrict the sum to range $-\Upsilon\le+\Delta\le\Upsilon$, where the choice of Υ depends on the desired accuracy of the calculation. With this truncation and using matrix notation, Eq. (2.5) becomes

$$\sum_{\Lambda=-\Upsilon}^{\Upsilon} H_{\Lambda,\Lambda+\Delta}C(\Lambda+\Delta)=0 . \quad (2.6)$$

Solving (2.6) for $C(\Lambda+\Upsilon)$, one gets

$$C(\Lambda+\Upsilon)=-H^{-1}_{\Lambda,\Lambda+\Upsilon}\sum_{\Lambda=-\Upsilon}^{\Upsilon-1} H_{\Lambda,\Lambda+\Delta}C(\Lambda+\Delta) . \quad (2.7)$$

Using Eq. (2.7) and the trivial identity $C(\Lambda+\Delta)=C(\Lambda+\Delta)$, a matrix equation of the following form is obtained:

$$\begin{bmatrix} C(\Lambda+1-\Upsilon) \\ C(\Lambda+2-\Upsilon) \\ \vdots \\ C(\Lambda+2\Upsilon-\Upsilon) \end{bmatrix} = T_\Lambda \begin{bmatrix} C(\Lambda-\Upsilon) \\ C(\Lambda+1-\Upsilon) \\ \vdots \\ C(\Lambda+2\Upsilon-1-\Upsilon) \end{bmatrix} , \quad (2.8)$$

where T_Λ is defined by

$$T_\Lambda=\begin{bmatrix} \underline{0} & \underline{1} & \underline{0} & \cdots & \underline{0} \\ \underline{0} & \underline{0} & \underline{1} & \cdots & \underline{0} \\ \vdots & \vdots & \underline{0} & \ddots & \underline{0} \\ \vdots & \vdots & \vdots & \vdots & \underline{1} \\ G_{\Lambda,\Lambda-\Upsilon} & G_{\Lambda,\Lambda+1-\Upsilon} & \cdots & \cdots & G_{\Lambda,\Lambda+2\Upsilon-1-\Upsilon} \end{bmatrix} . \tag{2.9}$$

Here $\underline{1}$ in general, is a nonsquare unit matrix and the matrices G in (2.9) are defined by

$$\begin{aligned} G_{\Lambda,\Lambda-\Upsilon}&=H^{-1}{}_{\Lambda,\Lambda+\Upsilon}H_{\Lambda,\Lambda-\Upsilon}\ , \\ G_{\Lambda,\Lambda+1-\Upsilon}&=H^{-1}{}_{\Lambda,\Lambda+\Upsilon}H_{\Lambda,\Lambda+1-\Upsilon}\ , \\ G_{\Lambda,\Lambda+2\Upsilon-1-\Upsilon}&=H^{-1}{}_{\Lambda,\Lambda+\Upsilon}H_{\Lambda,\Lambda+2\Upsilon-1-\Upsilon}\ , \end{aligned} \tag{2.10}$$

etc.

Now if in the $\hat{\mathbf{z}}$ direction the superlattice repeats itself every Γ number of planes, then from Bloch's theorem we have

$$\Psi(\mathbf{r}+d_\Gamma\hat{\mathbf{z}})=e^{ik_zd_\Gamma}\Psi(\mathbf{r})\ , \tag{2.11}$$

which in terms of expansion coefficients becomes

$$\begin{bmatrix} C(\Lambda-\Upsilon+\Gamma) \\ C(\Lambda+1-\Upsilon+\Gamma) \\ \vdots \\ C(\Lambda+\Upsilon-1+\Gamma) \end{bmatrix}=e^{ik_zd_\Gamma}\begin{bmatrix} C(\Lambda-\Upsilon) \\ C(\Lambda+1-\Upsilon) \\ \vdots \\ C(\Lambda+\Upsilon-1) \end{bmatrix} . \tag{2.12}$$

Using Eq. (2.8) Γ times, one can obtain the left-hand side of (2.10) as follows:

$$\begin{bmatrix} C(\Lambda-\Upsilon+\Gamma) \\ C(\Lambda+1-\Upsilon+\Gamma) \\ \vdots \\ C(\Lambda+\Upsilon-1+\Gamma) \end{bmatrix}=T^P_{\Lambda,\Gamma}\begin{bmatrix} C(\Lambda-\Upsilon) \\ C(\Lambda+1-\Upsilon) \\ \vdots \\ C(\Lambda+\Upsilon-1) \end{bmatrix} , \tag{2.13}$$

where

$$T^P_{\Lambda,\Gamma}\equiv T_{\Lambda+\Gamma}T_{\Lambda+\Gamma-1}\cdots T_{\Lambda+1}T_\Lambda\ . \tag{2.14}$$

Comparing (2.12) and (2.13) we get

$$T^P_{\Lambda,\Gamma}\begin{bmatrix} C(\Lambda-\Upsilon) \\ C(\Lambda+1-\Upsilon) \\ \vdots \\ C(\Lambda+\Upsilon-1) \end{bmatrix}=e^{ik_zd_\Gamma}\begin{bmatrix} C(\Lambda-\Upsilon) \\ C(\Lambda+1-\Upsilon+) \\ \vdots \\ C(\Lambda+\Upsilon-1) \end{bmatrix} . \tag{2.15}$$

To find the complex band structure for any desired energy and $\mathbf{k}_t$, the product matrix $T^P_{\Lambda,\Gamma}$ is diagonalized, and from the eigenvalues the values of k_z can be determined.

Note that for very-long-period superlattices many of the transfer matrices T_Λ, or perhaps products of a few of them, will repeat a number of time in the product (2.14). In such a case, the evaluation of the product $T^P_{\Lambda,\Gamma}$ can be simplified by first diagonalizing the repeating unit, constructing the product in that basis, and transforming back to the original basis. For such large-period superlattices, then, the difficulty in constructing the product transfer matrix is essentially independent of the superlattice period.

III. LINEAR COMBINATION OF GAUSSIAN ORBITALS (LCGO) METHOD

In the past the LCGO method has been used in calculating the band structures of a variety of bulk materials such as group-IV and -III-V semiconductors, insulators, metals, alloys, etc.[12–14] The advantage of employing the LCGO method over most other tight-binding approaches, which are empirical in nature, is that it can be implemented at either a semi–*ab initio* or *ab initio* level. Moreover, all the integrals involved in the evaluation of the Hamiltonian and overlap matrix elements can be carried out analytically. The details of this method as applied by Ching *et al.*[12] have been adequately discussed. Below, we give a summary of how we apply this method to our problem.

The effective potential of atoms of type A is fitted to the functional form

$$V^A(\mathbf{r})=-\frac{Z_A}{|\mathbf{r}|}e^{-\gamma_Ar^2}+\sum_i \mathcal{C}_i^Ae^{-\beta_i^Ar^2}=V_c^A+V_{\rm xc}^A\ . \tag{3.1}$$

In a fully-self-consistent calculation these effective potentials would be determined iteratively. Here, we simply use the semi–*ab initio* bulk silicon and germanium potentials. That is, as a first approximation we neglect any modification of these effective potentials due to the fact that the atoms reside in a superlattice rather than in a bulk crystal. Next, s-type ($e^{-\alpha_ir^2}$), p-type ($xe^{-\alpha_ir^2}$, etc.), and d-type ($xye^{-\alpha_ir^2}$, etc.) Gaussian orbitals are used to expand the atomic orbitals as follows:

$$\Phi^A_{pqs}(\mathbf{r})=\sum_n \mathcal{D}^A_{pqs,n}G^A(\alpha_n,\mathbf{r},p,q,s)\ , \tag{3.2}$$

where $G^A(\alpha_n,\mathbf{r},p,q,s)=x_A^py_A^qz_A^se^{-\alpha_nr_A^2}$ are the Gaussian functions and $\mathcal{D}^A_{pqs,n}$ are the expansion coefficients. Defining $i\equiv\{p,q,s\}$ as a collective index, we have

$$\Phi^A_i(\mathbf{r})=\sum_n \mathcal{D}^A_{i,n}G^A(\alpha_n,\mathbf{r},i)\ . \tag{3.3}$$

Here again, we adopt the bulk silicon and germanium expansion coefficients as a first approximation to the superlattice expansion coefficients. In a self-consistent calculation, these orbitals could be improved iteratively. The matrix elements $(H_{\Lambda,\Lambda+\Delta})_{i_\Lambda j_{\Lambda+\Delta}}$ in terms of these orbitals and the potential of the form even by (3.1) are presented in the Appendixes. Note that all the integrals involved in these expressions are performed analytically.

To simplify the calculation, we reduce the dimensions

TABLE I. Lattice constants in Å.

Substrate	$a_{\parallel}$	$a_{\perp}^{Si}$	$a_{\perp}^{Ge}$
Si	5.43	5.43	5.82

of our transfer matrices by orthogonalizing the valence Bloch state of each type of atom to the core states of *all* the atoms. In this smaller basis, the valence states of the different-type atoms are mixed, and we have the added advantage that all the matrices $H_{\Lambda,\Lambda+\Delta}$ are square. For example, within the minimal number of orbitals scheme we identify core and valence states of Si as $(1s,2s,2p)$ and $(3s,3p)$, respectively, while for Ge the core and valence states are $(1s,2s,2p,3s,3p,3d)$ and $(4s,4p)$, respectively. So a transfer matrix before orthogonalization includes four types of $H_{\Lambda,\Lambda+\Delta}$ matrices:

(i) the 9×9 matrices between two Si planes,
(ii) the 9×18 matrices between a Si plane and a Ge plane,
(iii) the 18×9 matrices between a Ge plane and a Si plane, and
(iv) the 18×18 matrices between two Ge planes.

By applying the orthogonalization procedure, we transform all these matrices to 4×4 matrices, as presented in the Appendixes. Note that this procedure is applicable regardless of whether minimal or extended number of orbitals are used, and that it can, of course, be used for more complicated superlattices. The product transfer matrix $T^{P}_{\Lambda,\Gamma}$ is then constructed and diagonalized. The result is a "first-order" complex band structure of the superlattice. In this paper we stop at this level. In a self-consistent calculation the eigenstates of $T^{P}_{\Lambda,\Gamma}$ are used to construct improved potentials and orbitals for the superlattice in a manner analogous to the procedure used in bulk calculations,[12] and the procedure is repeated to convergence.

IV. RESULTS AND DISCUSSION

In the present work, for a superlattice grown on a Si substrate we have used transverse and longitudinal lattice constants obtained from relying on the macroscopic Poisson's ratio, as described by Van de Walle *et al.*[15] and Hybertsen *et al.*[2] The Si—Ge bond length is taken to be the average of the cubic Si—Si and the strained Ge—Ge bond lengths. These values are summarized in Table I. Results of a self-consistent energy-minimization calculation[15] show that the above lattice spacings produce a superlattice geometry which is very close to the minimum-energy geometry.

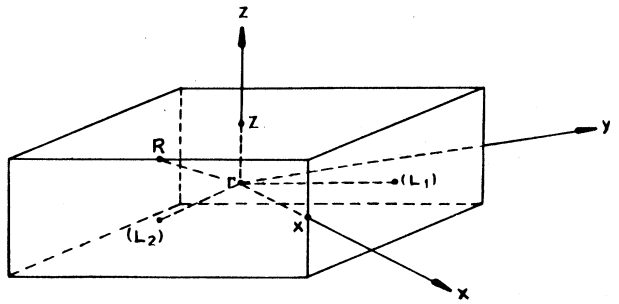

FIG. 1. The strained $(Si)_n/(Ge)_n$ superlattice Brillouin zone.

The potentials for bulk Si and Ge for simplicity have been obtained[12] from the $X\alpha$ method by adjusting α to give the correct band gaps of each bulk material. These bulk potentials are used to construct the superlattice potential as described in Sec. II B. In this manner we do not do any fitting to the superlattice properties. The superlattice potential is expanded over 17 planes (i.e., over each central plane Λ and eight planes on each side of it).

Here, for simplicity, we only present the real part of our complex bands. The real band structure of the superlattice is obtained from the complex band by requiring the eigenvalues $e^{ik_z d_\Gamma}$ to satisfy the conditions

$$[|\mathrm{Re}(e^{ik_z d_\Gamma})|+|\mathrm{Im}(e^{ik_z d_\Gamma})|]^{1/2}=1\ . \tag{4.1}$$

The real bands are then given by

TABLE II. Band gaps (from this calculation) for $(Si)_n/(Ge)_n$ superlattices.

Superlattice	Direct gap	Indirect gap
$(Si)_2/(Ge)_2$	1.86	0.78
$(Si)_3/(Ge)_3$	1.20	0.77
$(Si)_4/(Ge)_4$	1.38	0.78
$(Si)_5/(Ge)_5$	1.26	0.76

TABLE III. Band-gap and transition energy in eV for $(Si)_4/(Ge)_4$ from the present calculation along with corresponding experimental results from electroreflectance (ER) (Refs. 4 and 8) and photocurrent (PC) (Ref. 8) measurements and the quasiparticle (QP) calculation (Ref. 3).

	Present calc.	*QP*	ER[a]	PC[a]
E_g	0.78	0.85, 0.95	0.76, 0.76	0.78, 0.90
ZF[b]	1.38	1.24, 1.34	1.1, 1.25	
	2.05	1.76, 1.86	1.8	
E_0	2.43	2.4, 2.5	2.2, 2.3	
E_1	2.61	2.50, 2.55	2.45, 2.58	

[a]Two different samples were used.
[b]Transitions to zone-folded states at Γ.

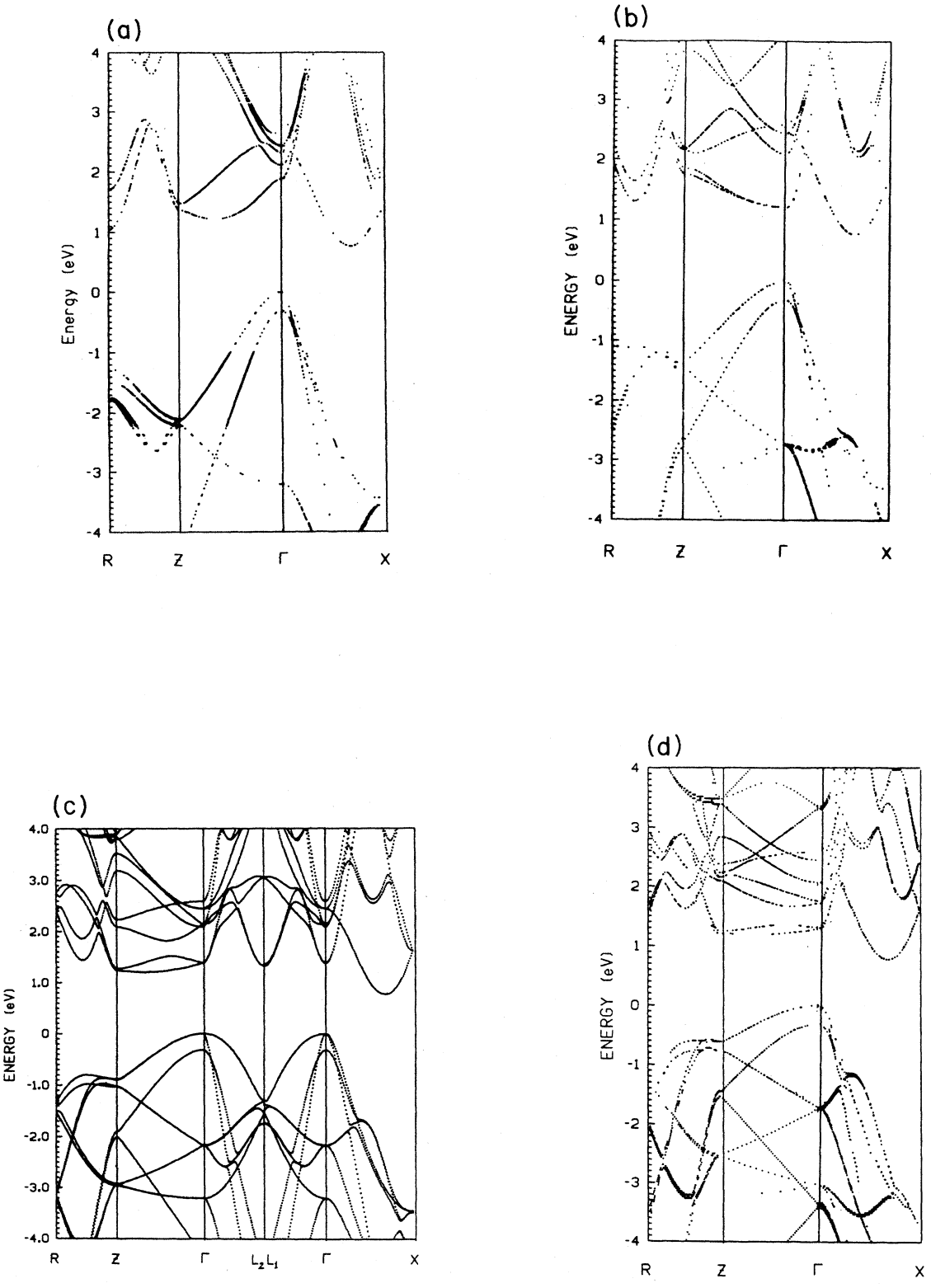

FIG. 2. Energy band structure of the strained $(Si)_n/(Ge)_n$ superlattices, (a) $(Si)_2/(Ge)_2$, (b) $(Si)_3/(Ge)_3$, (c) $(Si)_4/(Ge)_4$ (note that the interface bonds lift the fourfold symmetry about the crystal axis, rendering points L_1 and L_2 distinguishable), and (d) $(Si)_5/(Ge)_5$. Darker regions represent energy regions where finer energy and transverse-wave-vector mesh size where used.

$$k_z^{\text{real}} = \frac{A \cos[\text{Re}(e^{ik_z d_\Gamma})]}{d_\Gamma} . \quad (4.2)$$

But A cos is defined between 0 and π, therefore we must require the condition $0 \le k_z d_\Gamma \le \pi$. This, in terms of the eigenvalues, translates into

$$\text{Im}(e^{ik_z d_\Gamma}) \ge 0 . \quad (4.3)$$

Note that, for a chosen energy and fixed $\mathbf{k}_t = (k_x, k_y)$, any vector $\mathbf{k} = (k_x, k_y, k_z)$ specifying a point in the Brillouin zone that lies on a line parallel to the $\hat{\mathbf{z}}$ and passes through $(k_x, k_y, 0)$ specifies a real band as long as its $\hat{\mathbf{z}}$ component satisfies Eqs. (2.15), (4.1), (4.2), and (4.3). This means that, for a fixed energy and $\mathbf{k}_t$, we obtain all the possible solutions of k_z along this line in one calculation. In practice, a window size is established for conditions (4.1); typically, we required Eq. (4.1) to be satisfied to within 0.1%.

Since the main aim of the present work is to introduce the transfer-matrix method for superlattices, in this sample calculation we have chosen to work with the minimal number of orbitals LCGO (MLCGO) method to calculate the transfer-matrix elements. The advantage of using a minimal number of orbitals is that the size of the resulting matrices is small. However, as expected, MLCGO conduction bands even in bulk materials are not as good as the extended number of orbitals LCGO (ELCGO) calculations, since working in a larger vector space offers more flexibility regardless of whether the calculations are *ab initio* or semi–*ab initio*. For example, the ELCGO calculations of Wang *et al.*,[13] which employ 18 orbitals for Si ($1s, 2s, 2p, 3s, 3p, 3d, 4s, 4p$), produce bands that have very similar topology to corresponding pseudopotential bands obtained by employing a large number of plane waves. But the MLCGO calculation[12] using only nine orbitals ($1s, 2s, 2p, 3s, 3p$) results in conduction bands which, at some points of Brillouin zone, have considerably different topology than pseudopotential bands. This problem is even more drastic in superlattice calculations. A case in point is the small magnitude of the splitting of the first and second pairs of the zone-folded states of $(Si)_4/(Ge)_4$, at Γ, in the present calculation (see Fig. 2). With MLCGO we observe these splitting magnitudes to be about 0.01 and 0.03 eV, respectively, compared to others, e.g., Hybertsen *et al.*,[2] who get 0.1 and 0.2 eV. This discrepancy can be easily understood in terms of insufficiency of using a minimal number of orbitals.

For example, we consider the case of the pair of the zone-folded states near 2.1 eV. These states correspond to the two degenerate bulk states at the X point of Si and Ge. Our bulk calculations show that these states are degenerate because their corresponding wave functions transform into each other under a space-group operation $\delta_{4z} = \{C_{4z} | \frac{1}{4} a(1,1,1)\}$ which belongs to O_h^7 ($Fd3m$), the space group of the diamond structure.[16] Under this operation the atoms in plane $\Lambda = 0$ are moved to the positions of the atoms in plane $\Lambda = 1$, etc. Now in $(Si)_4/(Ge)_4$ this is not a symmetry operation because Si atoms in the plane $\Lambda = 3$ must be moved to the positions of the Ge atoms in $\Lambda = 4$ plane, etc. But note that atoms in planes $\Lambda = 0, 1, 2, 3, 5, 6, 7$, etc. are moved to positions in planes which originally were occupied by the same type of atoms. So, δ_{4z} is almost a symmetry operation of $(Si)_4/(Ge)_4$. Further note that, as the period of a superlattice increases, this operation gets closer to a true symmetry operation.

Thus the two superlattice wave functions corresponding to the degenerate bulk states do not quite transform into each other under this operation because the Bloch-state contributions to these wave functions from the planes $\Lambda = 4$, etc. do not transform properly. If the number of the valence orbitals on each atom from which the Bloch states are constructed is small, the difference between the two superlattice wave functions will not be much. However, if a larger number of valence orbitals for each atom is used, the difference can be expected to become greater and the near degeneracy to be removed further. Therefore, it is not surprising that in the present sample calculation, where we have utilized minimal sp^3-orthogonalized valence Bloch states, the resulting magnitudes are probably smaller than what they should be. We would expect to observe a better estimate of these magnitudes if the sp^3-orthogonalized valence Bloch states were augmented by, say, the inclusion of d-type valence states. Also note that, since in pseudopotential calculations of semiconductors the basis set typically consists of a large number of plane waves, it is perhaps not surprising that the splitting magnitudes should be closer to the true values.

The real band structures of $(Si)_n/(Ge)_n$ (001) superlattices for $n = 2-5$ along certain directions in the Brillouin zone (see Fig. 1) are given in Fig. 2. The direct and indirect band gaps are summarized in Table II. We find the gap for all of these superlattices to be indirect. Our results for the band-gap and direct-transition energies for $(Si)_4/(Ge)_4$ are in good agreement with experimental[3,5] and the quasiparticle (QP) calculation[2] results, as seen from Table III, despite the fact that our present calculation is not self-consistent.

To summarize, we have demonstrated that a real-space transfer-matrix method can be used to directly evaluate the complex and real band structures of superlattices. We plan to turn to applications involving the complex bands, to improving our bands through use of ELCGO and self-consistent calculations, and the calculation of optical properties using this approach, in future publications.

ACKNOWLEDGMENTS

We wish to thank Professor W. Y. Ching for providing us with his data for the tight-binding orbitals and potentials of bulk Si and Ge. We would also like to thank Dr. C. M. de Sterke for his helpful comments. We gratefully acknowledge research support from the Natural Sciences and Engineering Research Council (NSERC) of Canada. This work was partially supported by Ontario Laser and Lightwave Research Centre.

APPENDIX A: MATRIX ELEMENTS

The Hamiltonian matrix elements $(H_{\Lambda,\Lambda+\Delta})_{i_\Lambda j_{\Lambda+\Delta}}$ are of the form

$$
\begin{aligned}
(H_{\Lambda,\Lambda+\Delta})_{i_\Lambda j_{\Lambda+\Delta}} = \sum_{s(\Lambda,\Delta)} e^{i\mathbf{k}_t\cdot\mathbf{R}_s(\Lambda,\Delta)} \sum_m \sum_n \mathcal{D}_{i,m}\mathcal{D}_{j,n} \\
\times \Big[\int d\mathbf{r}\, G(\alpha_m,\mathbf{0},i)(-\tfrac{1}{2}\nabla^2) G(\alpha_n,\mathbf{R}_s(\Lambda,\Delta)-d_\Delta\hat{\mathbf{z}},j) \\
- \sum_{\Omega(\Lambda)} Z(\Lambda,\Omega) \sum_{t(\Lambda,\Omega)} \int d\mathbf{r}\, G(\alpha_m,\mathbf{0},i) \\
\times \frac{\exp\{-\beta(\Lambda,\Omega)[\mathbf{r}-\mathbf{R}_t(\Lambda,\Omega)-d_\Omega\hat{\mathbf{z}}]^2\}}{|\mathbf{r}-\mathbf{R}_t(\Lambda,\Omega)-d_\Omega\hat{\mathbf{z}}|} \\
\times G(\alpha_n,\mathbf{R}_s(\Lambda,\Delta)-d_\Delta\hat{\mathbf{z}},j) \\
+ \sum_{\Omega(\Lambda)} \sum_{t(\Lambda,\Omega)} \sum_u \mathcal{C}_u(\Lambda,\Omega) \int d\mathbf{r}\, G(\alpha_m,\mathbf{0},i) \\
\times \exp\{-\gamma_u(\Lambda,\Omega)[\mathbf{r}-\mathbf{R}_t(\Lambda,\Omega)-d_\Omega\hat{\mathbf{z}}]^2\} \\
\times G(\alpha_n,\mathbf{R}_s(\Lambda,\Delta)-d_\Delta\hat{\mathbf{z}},j) \\
- E\int d\mathbf{r}\, G(\alpha_m,\mathbf{0},i) G(\alpha_n,\mathbf{R}_s(\Lambda,\Delta)-d_\Delta\hat{\mathbf{z}},j) \Big] ,
\end{aligned}
\tag{A1}
$$

where $\Omega(\Lambda)$ labels different planes over which the potential is expanded, $s(\Lambda,\Delta)$ and $t(\Lambda,\Omega)$ give the number of two-dimensional vectors included in each plane, and other symbols are as defined in the text. Typically, we restrict the vectors to lie within a sphere of radius equivalent to eight nearest neighbors and centered at the origin of the plane Λ. All the integrals are performed analytically.

APPENDIX B: ORTHOGONALIZATION TO CORE BLOCH STATES

Let $|b_{\Lambda_+\Delta}\rangle_V$ be the abstract state representing the two-dimensional superlattice valence Bloch (VB) state $\xi_{i_{\Lambda+\Delta}\Lambda+\Delta}$ located in the $(\Lambda+\Delta)$th plane. Similarly, $|b_{\Lambda+\Omega}\rangle_C$ represents a core Bloch (CB) state in the $(\Lambda+\Omega)$th plane. Note that V and C differ from plane to plane, i.e., $V=V(\Lambda+\Delta)$ and $C=C(\Lambda+\Omega)$. We construct a new VB state $|b^0_{\Lambda+\Delta}\rangle_V$ as follows:

$$
|b^0_{\Lambda+\Delta}\rangle_V = |b_{\Lambda+\Delta}\rangle_V + \sum_{\Theta(\Lambda+\Delta)} \sum_{C'(\Lambda+\Delta,\Theta)} \mathcal{A}_{\Lambda+\Delta,V;\Lambda+\Theta,C'} |b_{\Lambda+\Theta}\rangle_{C'} ,
\tag{B1}
$$

where $\Theta(\Lambda+\Delta)$ runs over all the planes such that $\Lambda+\Delta-\Upsilon\le\Theta\le\Lambda+\Delta+\Upsilon$. The condition for orthogonality requires that

$$
\langle b^0_{\Lambda+\Delta}|b_{\Lambda+\Omega}\rangle_{VC} = 0 .
\tag{B2}
$$

Substituting (B1) into (B2) we get

$$
\langle b_{\Lambda+\Delta}|b_{\Lambda+\Omega}\rangle_{VC} + \sum_{\Theta(\Lambda+\Delta)} \sum_{C'(\Lambda+\Delta,\Theta)} \mathcal{A}^*_{\Lambda+\Delta,V;\Lambda+\Theta,C'} \langle b_{\Lambda+\Theta}|b_{\Lambda+\Omega}\rangle_{C'C} = 0 .
\tag{B3}
$$

To determine the coefficients $\mathcal{A}$, a series of simultaneous equations must be solved. However, since the overlap between different core states is small, we assume

$$
\langle b_{\Lambda+\Theta}|b_{\Lambda+\Omega}\rangle_{C'C} = \delta_{C',C}\delta_{\Theta,\Omega} .
\tag{B4}
$$

With the above approximation, (B3) gives

$$
\mathcal{A}^*_{\Lambda+\Delta,V;\Lambda+\Omega,C} = -\langle b_{\Lambda+\Delta}|b_{\Lambda+\Omega}\rangle_{VC} .
\tag{B5}
$$

Substituting (B5) into (B1), we get

$$
|b^0_{\Lambda+\Delta}\rangle_V = |b_{\Lambda+\Delta}\rangle_V - \sum_{\Theta(\Lambda+\Delta)} \sum_{C(\Lambda+\Delta,\Theta)} |b_{\Lambda+\Theta}\rangle_C \langle b_{\Lambda+\Theta}|b_{\Lambda+\Delta}\rangle_{CV} .
\tag{B6}
$$

In the actual calculation the orthogonalization procedure is applied to the matrix $H_{\Lambda,\Lambda+\Delta}$. In the new basis this matrix is given by

$$
\begin{aligned}
(H_{\Lambda,\Lambda+\Delta})_{V'V} &\equiv \langle b^0_\Lambda | H | b^0_{\Lambda+\Delta} \rangle_{V'V} \\
&= \langle b_\Lambda | H | b_{\Lambda+\Delta} \rangle_{V'V} - \sum_{\Omega(\Lambda)} \sum_{C(\Lambda,\Omega)} \langle b_\Lambda | H | b_{\Lambda+\Omega} \rangle_{V'C} \langle b_{\Lambda+\Omega} | b_{\Lambda+\Delta} \rangle_{CV} \\
&\quad - \sum_{\Theta(\Lambda)} \sum_{C'(\Lambda,\Theta)} \langle b_\Lambda | b_{\Lambda+\Theta} \rangle_{V'C'} \langle b_{\Lambda+\Theta} | H | b_{\Lambda+\Delta} \rangle_{C'V} \\
&\quad + \sum_{\Omega(\Lambda)} \sum_{C(\Lambda,\Omega)} \sum_{\Theta(\Lambda)} \sum_{C'(\Lambda,\Theta)} \langle b_\Lambda | b_{\Lambda+\Theta} \rangle_{V'C'} \langle b_{\Lambda+\Theta} | H | b_{\Lambda+\Omega} \rangle_{C'C} \langle b_{\Lambda+\Omega} | b_{\Lambda+\Delta} \rangle_{CV} \, . \qquad \text{(B7)}
\end{aligned}
$$

[1] R. People and S. A. Jackson, Phys. Rev. B **36**, 1310 (1987).

[2] M. S. Hybertsen and M. Schlüter, Phys. Rev. B **36**, 9683 (1987).

[3] T. P. Pearsall, J. Bevk, L. C. Feldman, J. M. Bonar, J. P. Mannaerts, and A. Ourmazd, Phys. Rev. Lett. **58**, 729 (1987); J. Bevk, A. Ourmazd, L. C. Feldman, T. P. Pearsall, J. M. Bonar, B. A. Davdson, and J. P. Mannaerts, Appl. Phys. Lett. **50**, 760 (1987).

[4] S. Froyen, D. M. Wood, and A. Zunger, Phys. Rev. B **36**, 4547 (1987); **37**, 6893 (1988).

[5] M. S. Hybertsen, M. Schlüter, R. People, S. A. Jackson, D. V. Lang, T. P. Pearsall, J. C. Bean, J. M. Vandenberg, and J. Bevk, Phys. Rev. B **37**, 10 195 (1988).

[6] I. Morrison and M. Jaros, Phys. Rev. B **37**, 916 (1988); K. B. Wong, M. Jaros, I. Morrison, and J. P. Hagon, Phys. Rev. Lett. **60**, 2221 (1988).

[7] The calculations in the following two papers are performed within empirical tight-binding and empirical pseudopotential methods, respectively, by L. Brey and C. Tejedor, Phys. Rev. Lett. **59**, 1022 (1987) and by M. A. Gell, Phys. Rev. B **34**, 7535 (1988).

[8] S. Circai and I. P. Batra, Phys. Rev. B **38**, 1835 (1988).

[9] J. N. Schülman and Y. C. Chang, Phys. Rev. B **27**, 2346 (1983).

[10] L. Brey and C. Tejedor, Phys. Rev. B **35**, 9112 (1987).

[11] M. S. Hybertsen and S. G. Louie, Phys. Rev. B **34**, 5390 (1986).

[12] M. Z. Huang and W. Y. Ching, J. Phys. Chem. Solids. **46**, 977 (1985), and references therein; W. Y. Ching and C. C. Lin, Phys. Rev. B **12**, 5536 (1975); W. Y. Ching, C. C. Lin, and D. L. Huber, *ibid.* **14**, 620 (1976); W. Y. Ching, Solid State Commun. **57**, 385 (1986); W. Y. Ching, Phys. Rev. B **34**, 2080 (1986).

[13] C. S. Wang and B. M. Klein, Phys. Rev. B **24**, 3393 (1981).

[14] B. N. Harmon, W. Weber, and D. R. Hamann, Phys. Rev. B **25**, 1109 (1982); M. Singh, C. S. Wang, and J. Callaway, *ibid.* **11**, 287 (1975); P. J. Feibelman, J. A. Appelbaum, and D. R. Hamann, *ibid.* **20**, 1433 (1979).

[15] C. G. Van de Walle and R. M. Martin, Phys. Rev. B **34**, 5621 (1986).

[16] M. Lax, *Symmetry Principles in Solid State and Molecular Physics* (Wiley, New York, 1974), Chap. 9.